HHS Public Access

Author manuscript

Neurobiol Dis. Author manuscript; available in PMC 2023 November 28.

Published in final edited form as:

Neurobiol Dis. 2023 November ; 188: 106326. doi:10.1016/j.nbd.2023.106326.

Regulation of extracellular progranulin in medial prefrontal cortex

Azariah K. Kaplelach,

Stephanie N. Fox,

Anna K. Cook,

Justin A. Hall,

Ryan S. Dannemiller,

Karen L. Jaunarajs,

Andrew E. Arrant*

Center for Neurodegeneration and Experimental Therapeutics, Alzheimer's Disease Center, Evelyn F. McKnight Brain Institute, Departments of Neurology and Neurobiology, University of Alabama at Birmingham, Birmingham, AL, USA

Abstract

Progranulin is a secreted pro-protein that has anti-inflammatory and neurotrophic effects and is necessary for maintaining lysosomal function. Mutations in progranulin (*GRN*) are a major cause of frontotemporal dementia. Most pathogenic *GRN* mutations cause progranulin haploinsufficiency, so boosting progranulin levels is a promising therapeutic strategy. Progranulin is constitutively secreted, then taken up and trafficked to lysosomes. Before being taken up from the extracellular space, progranulin interacts with receptors that may mediate anti-inflammatory and growth factor-like effects. Modifying progranulin trafficking is a viable approach to boosting progranulin, but progranulin secretion and uptake by cells in the brain is poorly understood and may involve distinct mechanisms from other parts of the body. Understanding the cell types and processes that regulate extracellular progranulin in the brain could provide insight into progranulin's mechanism of action and inform design of progranulin-boosting therapies. To address this question we used microdialysis to measure progranulin in interstitial fluid (ISF) of mouse medial prefrontal cortex (mPFC). $Grn^{+/-}$ mice had approximately 50% lower ISF progranulin than wild-type mice, matching the reduction of progranulin in cortical tissue.

*Corresponding author at: 1825 University Blvd., SHEL 1106, Birmingham, AL 35294, USA. andrewarrant@uabmc.edu (A.E. Arrant).

CRediT authorship contribution statement

Azariah K. Kaplelach: Investigation, Formal analysis, Writing - review & editing. **Stephanie N. Fox:** Investigation, Writing – review & editing. **Anna K. Cook:** Investigation, Formal analysis, Writing – review & editing. **Justin A. Hall:** Investigation, Writing – review & editing. **Ryan S. Dannemiller:** Investigation, Writing – review & editing. **Karen L. Jaunarajs:** Investigation, Formal analysis, Writing – review & editing. **Andrew E. Arrant:** Investigation, Formal analysis, Conceptualization, Writing - original draft, Writing - review & editing.

Declaration of Competing Interest

The authors declare that they have no competing interests.

Appendix A. Supplementary data

Supplementary data to this article can be found online at https://doi.org/10.1016/j.nbd.2023.106326.

Fluorescent *in situ* hybridization and immunofluorescence confirmed that microglia and neurons are the major progranulin-expressing cell types in the mPFC. Studies of conditional microglial (Mg-KO) and neuronal (N-KO) *Grn* knockout mice revealed that loss of progranulin from either cell type results in approximately 50% reduction in ISF progranulin. LPS injection (i.p.) produced an acute increase in ISF progranulin in mPFC. Depolarizing cells with KCl increased ISF progranulin, but this response was not altered in N-KO mice, indicating progranulin secretion by non-neuronal cells. Increasing neuronal activity with picrotoxin did not increase ISF progranulin. These data indicate that microglia and neurons are the source of most ISF progranulin in mPFC, with microglia likely secreting more progranulin per cell than neurons. The acute increase in ISF progranulin after LPS treatment is consistent with a role for extracellular progranulin in regulating inflammation, and may have been driven by microglia or peripheral immune cells. Finally, these data indicate that mPFC neurons engage in constitutive progranulin secretion that is not acutely changed by neuronal activity.

Keywords

Progranulin; Microglia; Secretion; Microdialysis

1. Introduction

Progranulin is a secreted pro-protein that is genetically associated with neurodegenerative disease and aging. Loss-of-function progranulin (*GRN*) mutations are one of the major autosomal dominant causes of frontotemporal dementia (FTD) (Baker et al., 2006; Cruts et al., 2006), and are associated with Lewy Body Dementia (Reho et al., 2022). *GRN* variants are also associated with risk for FTD (Rademakers et al., 2008), Alzheimer's disease (Lee et al., 2011; Perry et al., 2013; Sheng et al., 2014), and Parkinson's disease (Brouwers et al., 2007; Mateo et al., 2013; Nalls et al., 2019; Rovelet-Lecrux et al., 2008), as well as aging-related patterns of gene expression in the cerebral cortex (Rhinn and Abeliovich, 2017). Most pathogenic *GRN* mutations cause progranulin haploinsufficiency (Baker et al., 2006; Cruts et al., 2006; Finch et al., 2009; Meeter et al., 2016), though some mutations impair progranulin secretion and processing (Kleinberger et al., 2016; Shankaran et al., 2008; Wang et al., 2010). A common disease-associated *GRN* polymorphism is also associated with reduced progranulin levels (Rademakers et al., 2008). These data are consistent with an important role for progranulin in maintaining brain health with age, and suggest that even mild reduction of progranulin increases risk for neurodegenerative disease.

Progranulin has several functions that may explain its association with neurodegeneration and aging. It restrains inflammatory responses in microglia and macrophages (Lui et al., 2016; Martens et al., 2012; Yin et al., 2010). It also exerts neurotrophic effects, promoting neuronal survival and outgrowth (Gass et al., 2012; Van Damme et al., 2008). Finally, progranulin is necessary for maintaining lysosomal function, as individuals with loss-of-function mutations on both *GRN* alleles develop the lysosomal storage disorder Neuronal Ceroid Lipofuscinosis (Almeida et al., 2016; Huin et al., 2019; Smith et al., 2012).

Consistent with its essential role in lysosomal function, progranulin primarily localizes to lysosomes in most cell types. Progranulin lacks a typical lysosomal sorting signal, so a substantial proportion of newly-synthesized progranulin appears to be secreted (Kleinberger et al., 2016; Shankaran et al., 2008), though some progranulin may be directly trafficked to lysosomes through the endolysosomal pathway (Tran et al., 2023; Zhou et al., 2015). Secreted progranulin is taken up and trafficked to lysosomes through several pathways, including direct binding to sortilin (Hu et al., 2010) and co-trafficking with prosaposin *via* receptors such as the mannose-6-phosphate receptor and LRP1 (Nicholson et al., 2016; Zhou et al., 2015; Zhou et al., 2017b).

While in the extracellular space, progranulin can interact with several signaling receptors. Progranulin may act as a growth factor by signaling through receptors such as EphA2 (Neill et al., 2016) and Notch (Altmann et al., 2016). Extracellular progranulin also regulates inflammatory responses to injury (Zhu et al., 2002). This might be mediated by antagonism of TNF receptors (Tang et al., 2011), though progranulin's interaction with TNF receptors remains unclear (Chen et al., 2013; Etemadi et al., 2013; Lang et al., 2018; Wang et al., 2015). Progranulin also interacts with perlecan, a component of the extracellular matrix, which may serve as an additional factor regulating the activity of extracellular progranulin (Gonzalez et al., 2003).

In both the lysosomal and extracellular compartments, progranulin is cleaved by several proteases into granulins (Kessenbrock et al., 2008; Lee et al., 2017; Mohan, 2021; Suh et al., 2012; Zhou et al., 2017a; Zhu et al., 2002). In lysosomes, progranulin cleavage may activate progranulin, as granulins mimic progranulin's effects on lysosomal enzymes (Beel et al., 2017; Butler et al., 2019; Root et al., 2023) and persist in lysosomes longer than progranulin (Holler et al., 2017). The role of progranulin cleavage in the extracellular space is less clear, as some granulins have opposing effects on inflammation and cellular growth as progranulin (Plowman et al., 1992; Shoyab et al., 1990; Zhu et al., 2002), while other granulins mimic progranulin's promotion of neuronal growth (De Muynck et al., 2013; Hyung et al., 2019; Van Damme et al., 2008).

The mechanism(s) by which progranulin exerts its protective effects in the brain may therefore involve an interplay of extracellular and lysosomal progranulin and granulins. However, the mechanisms regulating levels of extracellular progranulin in the brain are poorly understood. Immunostaining and reporter mice indicate that neurons and microglia are the major cell types expressing progranulin in mouse brain (Petkau et al., 2010), though sequencing studies indicate that astrocytes and other cell types express progranulin to a higher degree than neurons (Saunders et al., 2018; Zhang et al., 2014). Microglia, neurons, and astrocytes secrete progranulin in culture (Davis et al., 2021; Elia et al., 2019; Martens et al., 2012; Suh et al., 2012), and presumably do so in brain, as progranulin is present in cerebrospinal fluid (CSF). CSF progranulin levels are reduced in *GRN* mutation carriers (Meeter et al., 2016), but comparison of blood and CSF progranulin levels indicate that different mechanisms may regulate extracellular progranulin in the central nervous system (CNS) than in the rest of the body (Nicholson et al., 2014; Wilke et al., 2016).

In this study, we used *in vivo* microdialysis in mouse medial prefrontal cortex (mPFC) to investigate the mechanisms regulating progranulin secretion in the brain. We investigated the contribution of CNS cell types to progranulin levels in interstitial fluid (ISF) and the response of ISF progranulin to stimuli such as systemic inflammation or local increases in neuronal activity.

2. Materials and methods

2.1. Animals

Grn$^{+/-}$ and *Grn*$^{-/-}$ mice (Jackson Laboratory #036771) (Martens et al., 2012) were compared to wild-type littermates for initial validation of progranulin microdialysis. Conditional *Grn* knockout mice were generated by crossing *Grn*$^{fl/fl}$ mice (Jackson Laboratory #036770) (Martens et al., 2012) with mice expressing *CaMKII*-Cre (Jackson Laboratory #005359) (Tsien et al., 1996) or *Cx3Cr1*-Cre-ER (Jackson Laboratory #020940) (Yona et al., 2013) to produce *Grn*$^{fl/fl}$:Cre+ or Cre− littermates. All mouse lines were maintained on a congenic C57Bl6/J background. Young adult mice were used for microdialysis studies, with most mice aged 2–6 months. *Cx3Cr1*-Cre-ER was induced by daily injections of 2 mg tamoxifen (MilliporeSigma) in 0.1 mL corn oil (MilliporeSigma) for five days, followed by a minimum wait of four weeks before microdialysis sampling to allow turnover of peripheral mono-nuclear cells (Goldmann et al., 2013). Mice were housed on a 12 h light/dark cycle with lights on from 6 AM to 6 PM in a facility accredited by the Association for Assessment and Accreditation of Laboratory Animal Care. Mice had free access to food (Envigo #7917) and water throughout the study, including during microdialysis sampling. All experiments were approved by the Institutional Animal Care and Use Committee of the University of Alabama at Birmingham.

2.2. In vitro microdialysis

Recombinant mouse progranulin (Adipogen) was diluted in artificial CSF (aCSF, 1.3 mM $CaCl_2$, 1.2 mM $MgSO_4$, 3 mM KCl, 0.4 mM KH_2PO_4, 25 mM $NaHCO_3$, 122 mM NaCl, pH 7.35. NaCl from Fisher Scientific, all other components from MilliporeSigma) supplemented with 4% bovine serum albumin (BSA, MilliporeSigma). Dilutions were made in low protein-binding tubes (ThermoFisher) to prevent progranulin from binding to the tubes (Gururaj et al., 2020), and post-experimental analysis revealed no detectable loss of progranulin due to non-specific binding to tubes. Progranulin concentrations for *in vitro* microdialysis were 1, 2, and 5 ng/mL, which approximates the range of concentrations reported in human cerebrospinal fluid (Batzu et al., 2020; Berghoff et al., 2016; De Riz et al., 2010; Meeter et al., 2016; Morenas-Rodriguez et al., 2016; Nicholson et al., 2014; Van Damme et al., 2008; Wilke et al., 2016).

Recombinant progranulin was sampled by microdialysis using 1000 kDa cut-off probes (Atmos LM, Amuza) (Takeda et al., 2011) with a 2 mm active membrane length. Microdialysis sampling was conducting using an Atmos (Amuza) protein microdialysis system, consisting of a syringe pump (Amuza #ESP-180LD) to push dialysate through the probe, a peristaltic pump (Amuza #ERP-10) to pull dialysate from the probe, and a refrigerated fraction collector (Amuza #FC-90) for sample collection. Probes were perfused

with aCSF supplemented with 4% BSA (MilliporeSigma) to maintain osmotic pressure (Trickler and Miller, 2003) and prevent progranulin from binding to the tubing (Gururaj et al., 2020). Each concentration of progranulin was measured with two one-hour samples at a flow rate of 1 μL/min, with a two-hour equilibration phase allowed when switching to each new concentration. Four independent probes were used for *in vitro* microdialysis.

2.3. In vivo microdialysis

Guide cannulae (4 mm length, Amuza) were implanted over the medial prefrontal cortex (right hemisphere) by stereotaxic surgery (coordinates from bregma: anterior +1.9 mm, lateral +0.4 mm, −1.0 mm ventral to the surface of the skull). Cannulae were secured to the skull with screws and dental cement (Stoelting) and kept patent by insertion of a 4 mm dummy cannula (Amuza). Mice were allowed to recover for a minimum of 48 h before microdialysis sampling, and only underwent sampling if fully recovered from surgery.

Microdialysis sampling was conducted as described above. The probes were designed so that the 2 mm membrane extended beyond the guide cannula, allowing sampling of ISF from the cingulate, prelimbic, and infralimbic cortices. This tissue sampled remained undisturbed until probe placement. The probe was connected to the system with a tether and liquid swivel that allowed mice to move freely throughout the experiment. During sampling, mice were housed in clear plastic chambers (30 cm L × 30 cm W × 35 cm high) outfitted with bedding, nesting material, and free access to food and water. The system was configured to sample simultaneously from two chambers, allowing parallel sampling from two experimental groups.

Microdialysis probes were placed the afternoon prior to sampling. Mice were briefly anesthetized with isoflurane to allow insertion of the probe, then placed in microdialysis chambers to recover. Probes were perfused with aCSF supplemented with 4% BSA as described above. Probes were perfused at 10 μL/min for at least 10 min to flush away any debris from insertion into the brain, then perfused at experimental flow rates for 8–12 h to allow equilibration with ISF prior to sampling.

Quantitative zero-flow microdialysis (Jacobson et al., 1985; Justice Jr., 1993) was conducted at flow rates ranging from 0.4 to 2 μL/min, with the initial equilibration phase conducted at 0.4 μL/min. All other experiments were conducted at a constant flow rate of 1 μL/min. Following equilibration, several hours of baseline samples were collected before administering treatments. LPS (Lipopolysaccharides from *Escherichia coli* O111:B4, MilliporeSigma #L2630) was administered by i.p. injection of 10 mg/kg LPS in 0.9% saline. Mice injected with saline served as the control group. Potassium was administered by perfusing aCSF with 100 mM KCl (MilliporeSigma) for one hour before switching back to standard aCSF (3 mM KCl as described above). Picrotoxin (Tocris) was dissolved in DMSO at 100 mM, then diluted in aCSF to a concentration of 100 μM and perfused through the probe for six hours. aCSF containing 0.01% DMSO served as the vehicle control.

Immediately following microdialysis sampling, mice were anesthetized with pentobarbital (200 mg/kg i.p., Euthasol, Virbac), the probe and guide cannula were removed, and mice were transcardially perfused with 0.9% saline. The brain was removed and cut into

hemibrains. The right hemibrain was post-fixed in 4% paraformaldehyde (MilliporeSigma). The left hemibrain was frozen on dry ice for analysis by ELISA or qPCR. Correct probe placement was confirmed by slicing the right hemibrain into 60 μm sections on a sliding microtome. Mice with incorrect probe placement or with excessive damage around the probe site were excluded from the study.

2.4. Progranulin ELISA

Progranulin levels in dialysate and brain tissue were determined by ELISA (Adipogen # AG-45A-0019YEK-KI01) according to the manufacturer's instructions. Microdialysis samples were diluted 1:1 with ELISA buffer prior to loading onto the ELISA plate. Brain tissue was prepared for ELISA by homogenizing in lysis buffer (50 mM Tris, 150 mM NaCl, 5 mM EDTA, 1% Triton X-100, 0.1% sodium deoxycholate) and centrifuging for 10 min at 5000 × *g*. Protein concentration of the supernatant was analyzed by BCA assay (ThermoFisher), and 40 μg of protein were loaded per well of the ELISA plate. ELISA signal was detected by reading absorbance using a Biotek Synergy LX plate reader. Concentrations of progranulin were determined based on a standard curve run on each plate.

To determine if the ELISA was capable of detecting granulins, 50 μg of recombinant mouse progranulin (Adipogen #AG-40A-0189Y) was cleaved overnight at 37 °C with 6 ng of recombinant human cathepsin L (R&D systems #952-CY-010) using a previously described protocol (Lee et al., 2017). For control samples, progranulin was incubated in reaction buffer without cathepsin L, or with cathepsin L and a protease inhibitor cocktail (Halt protease inhibitor cocktail, ThermoFisher #78429). After the reaction, complete cleavage was confirmed by SDS-PAGE on 10% polyacrylamide gels (Bio-Rad), followed by staining with Coomassie Fluor Orange (ThermoFisher). Samples were then diluted to 1 ng/mL progranulin in ELISA buffer and analyzed as described above.

2.5. Lactate assay

L-lactate levels in dialysate were determined using a kit (Biovision #K607/Abcam #ab65330) according to the manufacturer's instructions. Samples were diluted 1:5 in assay buffer, then analyzed using the manufacurer's protocol for colorimetric detection. Absorbance was read using a Biotek Synergy LX plate reader, and lactate concentrations were determined based on a standard curve run on each plate.

2.6. Magnetic-activated cell sorting (MACS)

Microglia, neurons, and astrocytes were isolated from mouse hemibrains by MACS, adapted from previously described methods (Bordt et al., 2020). For comparison of *Grn* in neurons, microglia, and astrocytes, a total of 6 mice were used. Brains from these mice were sliced at the midline to generate a total of 12 hemibrains, with each hemibrain assigned to isolation of one cell type. Mice were transcardially perfused with 0.9% saline, brains were removed, sliced into hemibrains, and immediately processed for MACS. Tissue was dissociated by digestion with 2 mg/mL Collagenase A (MilliporeSigma) and 0.5 mg/mL DNase I (MilliporeSigma) and trituration with a series of fire-polished pipettes (Bordt et al., 2020). After dissociation, samples were treated with debris removal solution (Miltenyi #130–109–398) according to the manufacturer's instructions. Microglia were isolated using anti-

Cd11b microbeads (Miltenyi #130–049–601), astrocytes were isolated using anti-ASCA-2 microbeads (Miltenyi #130–097–678), and neurons were isolated by negative selection using a mouse neuron isolation kit (Miltenyi #130–115–390). Microbead-bound cells were separated using a Quad-roMACS separator and LS columns (Miltenyi #130–091–051). After separation, cells were pelleted by centrifugation, then processed with Trizol reagent (ThermoFisher) for RNA isolation.

2.7. qPCR

RNA was isolated from frontal cortical tissue or MACS-purified cells using Trizol reagent (ThermoFisher). Samples were treated with DNase (Invitrogen TURBO DNA-free kit, ThermoFisher), then reverse transcribed using iScript reverse transcriptase (Bio-Rad). The resulting cDNA was analyzed by qPCR using PowerTrack SYBR green master mix (ThermoFisher) on a QuantStudio 3 system (ThermoFisher). Transcripts were analyzed with the following primers (Prime-Time, Integrated DNA Technologies): *Grn* (Mm.PT.58.16608371.g), *Tnf* (Mm. PT.58.12575861), *Il1b* (Mm.PT.58.41616450), *Rbfox3* (Mm. PT.58.32889417), *Itgam* (Mm.PT.58.14195622), *Cx3Cr1* (Mm. PT.58.17555544), *Tmem119* (Mm.PT.58.6766267), *Aldoc* (Mm. PT.58.43415246), *Gfap* (Mm.PT.58.6609337), *S100b* (Mm. PT.58.30112765), *Olig2* (Mm.PT.58.140319010), and *Plp1* (Mm. PT.58.28833929). Expression of transcripts was normalized to expression of *Gapdh* (F:GGGAAGCCCATCACCATCTT, R: GCCTTCTCCATGGTGGTGAA) or *Actb* (F: GGCTGTATTCCCCTCCATCG, R:CCAGTTGGTAACAATGCCATGT).

2.8. Small molecule fluorescent in situ hybridization (FISH)

FISH was performed as described previously (Fox et al., 2022) with the following modifications using the RNAscope Multiplex Fluorescent V2 Assay (Advanced Cell Diagnostics/ACD #323270). Mice were anesthetized with isoflurane and decapitated. Brains were removed and flash frozen on powdered dry ice. Brains were sliced into 20 μm sections on a cryostat, which were mounted onto SuperFront Plus slides (Fisher Scientific #1255015), immediately refrozen on dry ice, and stored at −80 °C until use. For the RNAscope V2 assay, tissue was fixed 15 min in 4% paraformaldehyde followed by dehydration with ethanol, then treated with hydrogen peroxide and protease III (ACD #322381). Next, slides were incubated with a mixture of RNAscope probes (*Grn* #539011 and either *C1qb* #438101-C3, *Rbfox3* #313311-C3, or *Gja1* #486191-C3, all from ACD) for 2h at 40°C followed by fluorescent amplification. After amplification steps, each channel was fluorescently labeled individually as follows: C1 probe (*Grn*): TSA Vivid Fluorophore 520 (ACD #323271) and C3 probe (*C1qb*, *Rbfox3*, or *Gja1*): TSA Vivid Fluorophore 570 (ACD #323272). Slides were coverslipped with Prolong Gold anti-fade mounting media containing DAPI (ThermoFisher).

2.9. Immunostaining

After transcardial perfusion of mice with 0.9% saline, brains were sliced into hemibrains and post-fixed for 48 h in 4% paraformaldehyde. Hemibrains were cryoprotected in 30% sucrose and sliced into 30 μm sections on a sliding microtome. Fluorescent immunostaining was conducted as previously described (Arrant et al., 2019). Brain sections were blocked in 3% BSA prior to overnight incubation with primary antibodies in 3% BSA. The following

primary antibodies were used: progranulin (R&D #AF2557, sheep polyclonal, 1:500), Iba1 (Wako #019–19,741, rabbit polyclonal), NeuN (MilliporeSigma #Abn91, chicken polyclonal, 1:1000), and S100β (Abcam #ab52642, rabbit monoclonal, 1:1000). Primary antibodies were then labeled with species-matched Alexa Fluor-conjugated secondary antibodies (ThermoFisher). Progranulin was labeled with Alexa Fluor 488 and cell markers were labeled with Alexa Fluor 594. After incubation with antibodies, all sections were stained with DAPI (ThermoFisher) and then with Sudan Black B (Acros Organics) to quench autofluorescence in the *Grn*$^{-/-}$ control sections.

2.10. Imaging and analysis

For comparison of progranulin intensity between CNS cell types and mouse genotypes, all sections were processed in parallel to avoid batch effects on intensity. Sections processed for FISH and immunofluorescence were imaged on a Nikon Ti2-C2 confocal microscope. 20× z-stacks were taken of the red (cell markers), green (progranulin), and blue (DAPI) channels. Laser and detector settings were adjusted so that no channel had saturated intensity, and were kept uniform for all images. Maximum intensity projections were generated for analysis of progranulin intensity within each cell type using Cell Profiler (Carpenter et al., 2006; Stirling et al., 2021).

Cell profiler was used to draw ROIs around the boundaries of each cell type. The following cell markers were used: for FISH, microglia (*C1qb*), neurons (*Rbfox3*), and astrocytes (*Gja1*); for immunofluorescence, microglia (Iba1), neurons (NeuN), and astrocytes (S100β). Signal for all protein markers, *C1qb*, and *Gja1* filled the cell body sufficiently that ROIs were drawn using these signals. *Rbfox3* exhibited a punctate signal, so *Rbfox3*+ DAPI nuclear profiles were used to draw ROIs for neurons in FISH sections. These ROIs were overlaid onto the green channel (progranulin), and the fluorescent intensity within each cell was measured. For all cell types, *Grn*$^{-/-}$ sections were run in parallel and used to correct for background fluorescence. For comparison of CNS cell types, integrated intensity (mean fluorescent intensity × ROI area) was analyzed due to size differences between cell types. The integrated intensity of cell types from each mouse was normalized to microglial intensity from the same mouse to correct for individual differences in fluorescent intensity. For comparison of microglial and neuronal progranulin intensity in conditional knockout mice, the mean progranulin intensity was analyzed due to similar cell sizes between groups.

2.11. Statistics

in vitro microdialysis data were analyzed by Pearson correlation. Progranulin levels in cortical tissue or ISF of mouse lines were analyzed by *t*-test. Progranulin transcript in MACS-sorted CNS cell types was analyzed by one-way ANOVA followed by Tukey's post-hoc test, and in MACS-sorted microglia from Mg-KO mice by two-way ANOVA (factors of cell type and Cre) followed by Sidak's post-hoc test. Progranulin intensity in CNS cell types was analyzed by nested (by mouse) one-way ANOVA, followed by Tukey's post-hoc test. Cellular progranulin intensity in conditional *Grn* knockout mice was analyzed by nested *t*-test. ISF progranulin from zero flow curves was calculated using a one-phase decay curve with least squares fit. Time-course analyses of ISF progranulin after treatment with LPS, KCl, or picrotoxin were conducted with repeated measures ANOVA, or mixed

effects analysis for data with missing values, as noted in the figure legends. LPS data were analyzed for an effect of sex using three-way repeated measures ANOVA (factors of treatment, sex, and time), with Greenhouse-Geisser correction. Since no effect or interaction of sex was observed, a lower-order two-way ANOVA was then conducted with factors of treatment and time and followed by Sidak's post-hoc test. Analysis of the average baseline *versus* treated ISF progranulin levels from these experiments was performed by paired *t*-test for KCl, or by two-way repeated measures ANOVA (factors of treatment/genotype and time) followed by Sidak's post-hoc test for LPS, picrotoxin, and KCl in N-KO mice. Comparisons of tissue cytokine and progranulin levels after LPS and the change in progranulin after KCl infusion in N-KO mice were performed by *t*-test.

For all analyses, two-tailed *p* values were calculated with α set at 0.05. Due to unequal variance, progranulin transcript and protein levels in CNS cell types and levels of cytokines and progranulin in tissue of LPS-treated mice were log-transformed prior to analysis. All analyses were performed with GraphPad Prism 9, except for three-way ANOVA, which was performed with IBM SPSS Statistics 27.

3. Results

3.1. Validating progranulin microdalysis

We established a microdialysis protocol for measuring ISF progranulin using a push-pull pump system and probes with a 1000 kDa cut-off membrane (Takeda et al., 2011). Progranulin was measured using an ELISA that detected progranulin, but only weakly detected granulins (Fig. S1). Reported values of progranulin in human cerebrospinal fluid range from around 0.7 to 6 ng/mL (Batzu et al., 2020; Berghoff et al., 2016; De Riz et al., 2010; Meeter et al., 2016; Morenas-Rodriguez et al., 2016; Nicholson et al., 2014; Van Damme et al., 2008; Wilke et al., 2016). We therefore conducted *in vitro* microdialysis to assess our ability to detect progranulin in this range. We found a consistent relationship of the progranulin recovered by microdialysis from samples ranging in concentration from 1 to 5 ng/mL (Fig. 1a), with a similar percent recovery across these concentrations (Fig. 1b).

When beginning *in vivo* microdialysis, we considered the effect of inflammation around the probe site. Brain injury in mice increases progranulin expression, though this response occurs between 1 and 4–5 days after injury (Menzel et al., 2017; Tanaka et al., 2013). Consistent with these prior studies, we found that progranulin levels did not dramatically increase within the first 24 h after probe placement (Fig. 1c), achieving a roughly stable baseline within 8–9 h after probe placement. In some instances, we observed dramatic increases in progranulin at time points longer than 24 h after probe placement. We therefore conducted experiments between 8 and 24 h after placing microdialysis probes.

3.2. $Grn^{+/-}$ mice have approximately half of wild-type ISF progranulin levels

As a final validation step, we compared ISF progranulin levels in wild-type and $Grn^{+/-}$ mice. $Grn^{+/-}$ mice had approximately 50% lower levels of ISF progranulin than wild-type littermates (Fig. 1d, e), which was consistent with roughly 50% loss of *Grn* mRNA (Fig.

1f) and progranulin protein (Fig. 1g) in frontal cortical tissue. Analysis of ISF from several *Grn*$^{-/-}$ mice revealed no detectable progranulin.

3.3. Analysis of progranulin expression in cell types of the mPFC

We next used microdialysis to investigate the contributions of various CNS cell types to ISF progranulin. A study using reporter mice and immunostaining found that microglia and neurons are the major progranulin-expressing cell types in the CNS (Petkau et al., 2010). However, sequencing-based analyses indicate much higher expression of progranulin in microglia, and in some cases astrocytes and other cell types, than neurons (Saunders et al., 2018; Zhang et al., 2014). We therefore used several approaches to assess progranulin expression in microglia, neurons, and astrocytes. Analysis of *Grn* transcript in microglia, neurons, and astrocytes isolated from dissociated brain tissue using MACS (Fig. S2) revealed much higher *Grn* expression in microglia than neurons and astrocytes, which both exhibited low *Grn* expression (Fig. 2a).

However, analysis of *in situ* progranulin expression produced a different pattern of results. Fluorescent *in situ* hybridization (FISH) for progranulin and markers of microglia, neurons, and astrocytes in mouse mPFC (Fig. 2b, c) revealed high levels of *Grn* transcript in microglia, with somewhat lower levels in neurons, and much lower levels in astrocytes. Similarly, immunofluorescence (Fig. 2d, e) revealed that of these cell types, microglia contained the most progranulin protein, with neurons having somewhat lower levels, and astrocytes having even lower levels of progranulin protein.

Collectively these data indicate that tissue dissociation may activate microglia, resulting in higher than normal progranulin expression. They also reveal a clear order of progranulin expression levels, with microglia expressing the highest levels, followed by neurons, and then astrocytes, which exhibited low levels of progranulin transcript and protein. We therefore focused our microdialysis experiments on microglia and neurons.

3.4. Microglia and CNS-resident macrophages contribute a significant portion of ISF progranulin in mPFC

We assessed the contribution of microglia and CNS-resident macrophages to ISF progranulin using *Grn*$^{fl/fl}$:*Cx3Cr1*-Cre-ER (Mg-KO) mice. Mg-KO mice and Cre− littermates were treated with tamoxifen or vehicle at least four weeks prior to microdialysis sampling to allow for turnover of peripheral monocytes (Goldmann et al., 2013). Consistent with prior data on Mg-KO mice (Krabbe et al., 2017), we found selective depletion of *Grn* transcript from Cd11b+ cells isolated by MACS (Fig. 3a, Fig. S3). Analysis of progranulin protein levels with immunofluorescence also revealed a strong depletion of progranulin from Iba1+ cells (Fig. 3b–d). Mg-KO mice exhibited significant reduction in *Grn* transcript (Fig. 3e) and progranulin protein (Fig. 3f) in frontal cortical tissue, confirming that microglia and CNS-resident macrophages are a significant source of progranulin in the frontal cortex. Finally, Mg-KO mice had a nearly 50% reduction in ISF progranulin levels (Fig. 3g, h), showing that microglia and CNS-resident macrophages are a significant source of extracellular progranulin in the mPFC.

3.5. Excitatory neurons contribute a significant portion of ISF progranulin in mPFC

We also assessed the contribution of excitatory neurons to ISF progranulin in the mPFC using *Grn*$^{fl/fl}$:*CaMKII*-Cre (N-KO) mice. As previously reported (Arrant et al., 2017), *CaMKII*-Cre depleted neuronal progranulin in frontal cortex (Fig. 4a, b). Despite the fact that *CaMKII*-Cre only targets excitatory neurons (Tsien et al., 1996), distribution analysis showed that nearly 90% of NeuN+ cells exhibited >50% loss of progranulin relative to the average control neuron (Fig. 4c). This loss of neuronal progranulin resulted in significant reduction of total tissue *Grn* transcript (Fig. 4d) and progranulin protein (Fig. 4e) in frontal cortex. N-KO mice also had a roughly 50% reduction of ISF progranulin on average (Fig. 4f, g), showing that excitatory neurons are a significant source of extracellular progranulin in the mPFC.

3.6. Inflammation increases ISF progranulin in mPFC

We next investigated processes that might alter progranulin secretion in the brain. Patients with inflammatory conditions exhibit elevated levels of progranulin in CSF (Berghoff et al., 2016; Kimura, 2017; Vercellino et al., 2011), so we investigated the effects of systemic inflammation on ISF progranulin in the mPFC.

Systemic administration of lipopolysaccharide (LPS) activates microglia (Hoogland et al., 2015) and increases levels of inflammatory cytokines in ISF within a few hours of injection (Takeda et al., 2011). To determine if injection of LPS would also induce an acute increase in ISF progranulin in mPFC, we administered a single dose of 10 mg/kg, i.p. of LPS and measured ISF progranulin for the following six hours.

LPS significantly increased ISF progranulin relative to saline-injected mice (Fig. 5a, b). Progranulin levels increased over the sampling period, reaching a peak of around 2.5-fold higher than baseline. LPS-treated mice exhibited robust increases in *Tnf* and *Il1b* expression in the contralateral frontal cortex (Fig. 5c, d), confirming an inflammatory response to LPS. However, the increase in ISF progranulin was not associated with an increase in *Grn* transcript (Fig. 5e) or protein levels (Fig. 5f) in frontal cortical tissue. While some mice did seem to show increased tissue progranulin levels, the increase in ISF progranulin was not significantly correlated with levels of *Grn* transcript ($r = -0.2915$, $p = 0.3339$) or progranulin protein ($r = -0.4031$, $p = 0.1939$) in the contralateral hemisphere.

While collecting LPS data, we noticed that the LPS-treated group contained a mix of mice with robust increases in ISF progranulin and mice with almost no change in ISF progranulin (Fig. 5b). Given recent reports of sex differences in microglia and other immune responses in progranulin knockout mice (Houser et al., 2022; Zhang et al., 2023), we powered this study to compare the LPS response in male and female mice. However, we did not observe a significant sex difference in LPS response (Fig. S4), and both sexes included a mix of "responder" and "non-responder" mice. We do not anticipate that this variability was due to inconsistent LPS injections, as all mice showed robust cytokine increases in mPFC from the contralateral hemisphere (Fig. 5c, d).

3.7. Stimulation of neuronal activity does not increase ISF progranulin in mPFC

We then investigated whether increases in neuronal activity might increase levels of ISF progranulin in mPFC. Progranulin promotes neuronal growth and survival (Gass et al., 2012; Ryan et al., 2009; Van Damme et al., 2008), and neuronal activity may increase secretion of progranulin in cultured neurons (Petoukhov et al., 2013). We began by depolarizing cells near the probe by infusing aCSF with a high concentration of potassium chloride (100 mM KCl). Infusion of aCSF with high-KCl immediately increased ISF progranulin (Fig. 6a, b), which returned to baseline over several hours. We confirmed that this was associated with an increase in activity by measuring levels of lactate in ISF (Fig. 6c, d) (Yamada et al., 2014), though lactate levels increased more slowly than progranulin levels.

To determine if the response to KCl indicated that neuronal activity increases ISF progranulin, we infused picrotoxin (100 μM) through the probe to disinhibit neuronal activity. In contrast to KCl infusion, 100 μM picrotoxin failed to increase ISF progranulin (Fig. 7a, b), despite the fact that this dose of picrotoxin robustly increased ISF lactate (Fig. 7c, d), indicating an increase in neuronal activity.

Given the lack of increase in ISF progranulin with infusion of picrotoxin, we hypothesized that the increase in ISF progranulin observed after 100 mM KCl might be mediated by non-neuronal cells. To test this hypothesis, we infused 100 mM KCl into N-KO mice and Cre–littermates. We observed no difference in the response to KCl between groups (Fig. 7e–g), indicating that this KCl response was not mediated by excitatory neurons in the mPFC. Given the dramatic overall loss of neuronal progranulin in *CaMKII*-Cre + mice (Fig. 4a–c), the KCl response may be driven instead by non-neuronal cells.

4. Discussion

In this study, we report that microglia and neurons are major contributors to ISF progranulin in the mPFC. Microglia, neurons, and astrocytes have been reported to express progranulin in the central nervous system and in culture (Elia et al., 2019; Martens et al., 2012; Petkau et al., 2010; Saunders et al., 2018; Suh et al., 2012; Zhang et al., 2014). Of these cell types, we confirmed that under normal conditions in the mPFC, microglia express the most progranulin per cell, followed by neurons, then astrocytes, which have low expression of progranulin (Fig. 2). Consistent with this expression pattern, microglia appear to secrete more progranulin than neurons into ISF, as Mg-KO and N-KO mice have roughly similar loss of ISF progranulin despite the lower abundance of microglia than neurons in mPFC. Based on the decrease in ISF progranulin from Mg-KO and N-KO mice (nearly 50% in each line), we infer that most ISF progranulin in mPFC is secreted from microglia and neurons. We also report that induction of systemic inflammation, but not stimulation of neuronal activity, acutely increases ISF progranulin levels.

In addition to the reduction of ISF progranulin in conditional *Grn* knockout mice, we observed roughly 50% reduction of ISF progranulin in $Grn^{+/-}$ mice. This 50% loss of progranulin closely matched the reduction of tissue progranulin levels in $Grn^{+/-}$ mice, showing no sign of a compensatory increase in progranulin secretion in the mPFC. This is consistent with human data, in which heterozygous *GRN* mutation carriers have reduced

CSF progranulin (Meeter et al., 2016), as do carriers of the *GRN* rs5848 T allele (Nicholson et al., 2014). Collectively, these data indicate that extracellular progranulin levels are closely associated with progranulin expression in the surrounding tissue, and may be determined by constitutive secretion of progranulin from the trans-Golgi network.

The increase in ISF progranulin after systemic LPS treatment is consistent with data showing that people with inflammatory conditions have elevated CSF progranulin (Berghoff et al., 2016; Kimura, 2017; Vercellino et al., 2011), and with data showing a role for extracellular progranulin in regulating inflammation (Zhu et al., 2002). However, our data do not allow us to determine the cellular source of this progranulin. The increase in ISF progranulin after LPS might be driven by increased progranulin secretion from activated microglia, as systemic LPS treatment activates microglia (Hoogland et al., 2015) and activated microglia and macrophages have increased progranulin expression (Ma et al., 2017; Naphade et al., 2010; Tanaka et al., 2013).

However, while cytokine expression indicated that all LPS-treated mice mounted an immune response in mPFC, we did not observe a significant increase in tissue progranulin expression. This data is consistent with microglial activation in the mPFC, but not with robust increases in microglial progranulin expression. A prior study with mice also found no change in brain tissue progranulin levels 6 h after LPS treatment, but did observe increased progranulin 24 h after LPS injection (Ma et al., 2017). Another study reported that serum progranulin is elevated 6 h after LPS injection (Yu et al., 2016). Thus, progranulin from peripheral immune cells may have crossed the blood brain barrier and contributed to the acute increase in ISF progranulin of LPS-treated mice. It is possible that microdialysis sampling conducted at least 24 h after LPS injection might reveal more robust and consistent increases in ISF progranulin, based on the report of increased progranulin expression in microglia at this time point (Ma et al., 2017).

Our data indicate that synaptic activity and neuronal depolarization do not acutely increase ISF progranulin levels. This stands in contrast to neurotrophic factors such as BDNF and NGF, which exhibit activity-dependent secretion from neurons (Blochl and Thoenen, 1995; Griesbeck et al., 1999). A previous study reported activity-dependent secretion of progranulin from cultured hippocampal neurons (Petoukhov et al., 2013). Our data indicate that if mPFC neurons do engage in activity-dependent secretion of progranulin, they do not do so on a scale that produces detectable changes in ISF progranulin. Instead, our data are consistent with mPFC neurons engaging in low-level constitutive progranulin secretion that does not significantly change with neuronal activity. It is also possible that there are regional differences in neuronal progranulin secretion, or in progranulin secretion from neurons in culture *versus in vivo*.

This study provides insight into previously reported effects of selective progranulin overexpression and knockdown in mouse models. Overexpressing progranulin in neurons improves not only neuronal lipofuscinosis, but also microglial reactivity in $Grn^{-/-}$ mice (Arrant et al., 2018b). This may be due to neuronal progranulin secretion and subsequent uptake by microglia. Additionally, conditional knockout of progranulin from either microglia (Arrant et al., 2018a; Krabbe et al., 2017; Petkau et al., 2017b) or neurons (Arrant

et al., 2018a; Arrant et al., 2017; Petkau et al., 2017a) fails to recapitulate the full microglial or neuronal phenotypes of *Grn*$^{-/-}$ mice, perhaps because the targeted cell type still has access to progranulin secreted by non-targeted cells.

This study primarily focused on progranulin secretion by microglia and neurons, but microdialysis is also a useful technique for analyzing other processes regulating levels of extracellular progranulin. Microdialysis studies have already confirmed that blocking progranulin uptake by sortilin increases levels of ISF progranulin (Kurnellas, 2023; Miyakawa et al., 2020), which is consistent with data from cultured cells and sortilin knockout mice (Hu et al., 2010; Lee et al., 2014). Progranulin also binds to perlecan (Gonzalez et al., 2003), raising the possibility of an extracellular pool of progranulin bound to the extracellular matrix. Microdialysis could help determine the functional consequences of this interaction. Progranulin's binding to the extracellular matrix may also provide a caveat to our finding that stimulating neuronal activity does not acutely increase ISF progranulin, as there might be small increases in secreted progranulin that bind to nearby cells and are not available for detection in ISF.

A limitation of this study is the lack of data on granulins in ISF, as the ELISA used to analyze microdialysis samples exhibited dramatic loss of signal after cleavage of progranulin into granulins (Fig. S1). Progranulin is cleaved into granulins both extracellularly (Kessenbrock et al., 2008; Mohan, 2021; Suh et al., 2012; Zhu et al., 2002) and in lysosomes (Lee et al., 2017; Zhou et al., 2017a). Granulins are also secreted (Holler et al., 2017), perhaps directly by lysosomes (Davis et al., 2021), and the ratio of granulins to progranulin may differ between brain regions (Zhang et al., 2022). There may therefore be changes in ISF granulins after inflammation or neuronal activity that are distinct from changes in ISF progranulin.

5. Conclusions

Using *in vivo* microdialysis, this study shows that microglia and neurons are major sources of ISF progranulin in mPFC. Based on analysis of cellular progranulin expression and ISF progranulin in conditional knockout mice, microglia express more progranulin than neurons and likely secrete more progranulin than neurons. ISF progranulin levels increase within a few hours of the onset of systemic inflammation due to LPS, despite a lack of detectable increase in progranulin in cortical tissue. In contrast, stimulating neuronal activity or directly depolarizing neurons failed to increase ISF progranulin. These data are consistent with studies showing an important role for progranulin in regulating inflammation in microglia (Krabbe et al., 2017; Lui et al., 2016; Martens et al., 2012; Zhang et al., 2020), but also show that neurons are a significant source of extracellular progranulin in the mPFC.

Supplementary Material

Refer to Web version on PubMed Central for supplementary material.

Acknowledgements

We thank Kelsey Greathouse and Jeremy Herskowitz for assistance with imaging.

Funding

This work was supported by the National Institute on Aging grants R00AG056597, R21AG068658, and P20AG068024.

Data availability

Data are available from the corresponding author upon request.

Abbreviations:

CNS	central nervous system
CSF	cerebrospinal fluid
FTD	frontotemporal dementia
GRN	progranulin
ISF	interstitial fluid
LPS	lipopolysaccharide
mPFC	medial prefrontal cortex
Mg-KO	microglial progranulin knockout mice (*Grn*$^{fl/fl}$:*Cx3Cr1*-CreER+)
N-KO	neuronal progranulin knockout mice (*Grn*$^{fl/fl}$:*CaMKII*-Cre+)

References

Almeida MR, et al. , 2016. Portuguese family with the co-occurrence of frontotemporal lobar degeneration and neuronal ceroid lipofuscinosis phenotypes due to progranulin gene mutation. Neurobiol. Aging 41 (200), e1–e5.

Altmann C, et al. , 2016. Progranulin promotes peripheral nerve regeneration and reinnervation: role of notch signaling. Mol. Neurodegener 11, 69. [PubMed: 27770818]

Arrant AE, et al. , 2017. Restoring neuronal progranulin reverses deficits in a mouse model of frontotemporal dementia. Brain 140, 1447–1465. [PubMed: 28379303]

Arrant AE, et al. , 2018a. Reduction of microglial progranulin does not exacerbate pathology or behavioral deficits in neuronal progranulin-insufficient mice. Neurobiol. Dis 124, 152–162. [PubMed: 30448285]

Arrant AE, et al. , 2018b. Progranulin gene therapy improves lysosomal dysfunction and microglial pathology associated with frontotemporal dementia and neuronal ceroid Lipofuscinosis. J. Neurosci 38, 2341. [PubMed: 29378861]

Arrant AE, et al. , 2019. Impaired beta-glucocerebrosidase activity and processing in frontotemporal dementia due to progranulin mutations. Acta Neuropathol. Commun 7, 218. [PubMed: 31870439]

Baker M, et al. , 2006. Mutations in progranulin cause tau-negative frontotemporal dementia linked to chromosome 17. Nature 442, 916–919. [PubMed: 16862116]

Batzu L, et al. , 2020. Cerebrospinal fluid progranulin is associated with increased cortical thickness in early stages of Alzheimer's disease. Neurobiol. Aging 88, 61–70. [PubMed: 31980280]

Beel S, et al. , 2017. Progranulin functions as a cathepsin D chaperone to stimulate axonal outgrowth in vivo. Hum. Mol. Genet 26, 2850–2863. [PubMed: 28453791]

Berghoff M, et al. , 2016. Quantification and regulation of the adipokines resistin and progranulin in human cerebrospinal fluid. Eur. J. Clin. Investig 46, 15–26. [PubMed: 26509463]

Blochl A, Thoenen H, 1995. Characterization of nerve growth factor (NGF) release from hippocampal neurons: evidence for a constitutive and an unconventional sodium-dependent regulated pathway. Eur. J. Neurosci 7, 1220–1228. [PubMed: 7582095]

Bordt EA, et al. , 2020. Isolation of microglia from mouse or human tissue. STAR Protoc 1.

Brouwers N, et al. , 2007. Alzheimer and Parkinson diagnoses in progranulin null mutation carriers in an extended founder family. Arch. Neurol 64, 1436–1446. [PubMed: 17923627]

Butler VJ, et al. , 2019. Multi-Granulin domain peptides bind to pro-Cathepsin D and stimulate its enzymatic activity more effectively than Progranulin in vitro. Biochemistry 58, 2670–2674. [PubMed: 31099551]

Carpenter AE, et al. , 2006. CellProfiler: image analysis software for identifying and quantifying cell phenotypes. Genome Biol 7, R100. [PubMed: 17076895]

Chen X, et al. , 2013. Progranulin does not bind tumor necrosis factor (TNF) receptors and is not a direct regulator of TNF-dependent signaling or bioactivity in immune or neuronal cells. J. Neurosci 33, 9202–9213. [PubMed: 23699531]

Cruts M, et al. , 2006. Null mutations in progranulin cause ubiquitin-positive frontotemporal dementia linked to chromosome 17q21. Nature 442, 920–924. [PubMed: 16862115]

Davis SE, et al. , 2021. Delivering progranulin to neuronal lysosomes protects against excitotoxicity. J. Biol. Chem 297, 100993. [PubMed: 34298019]

De Muynck L, et al. , 2013. The neurotrophic properties of progranulin depend on the granulin E domain but do not require sortilin binding. Neurobiol. Aging 34, 2541–2547. [PubMed: 23706646]

De Riz M, et al. , 2010. Cerebrospinal fluid progranulin levels in patients with different multiple sclerosis subtypes. Neurosci. Lett 469, 234–236. [PubMed: 19963041]

Elia LP, et al. , 2019. Genetic regulation of neuronal Progranulin reveals a critical role for the autophagy-lysosome pathway. J. Neurosci 39, 3332–3344. [PubMed: 30696728]

Etemadi N, et al. , 2013. Progranulin does not inhibit TNF and lymphotoxin-alpha signalling through TNF receptor 1. Immunol. Cell Biol 91, 661–664. [PubMed: 24100384]

Finch N, et al. , 2009. Plasma progranulin levels predict progranulin mutation status in frontotemporal dementia patients and asymptomatic family members. Brain 132, 583–591. [PubMed: 19158106]

Fox SN, et al. , 2022. Estrogen-related receptor gamma regulates mitochondrial and synaptic genes and modulates vulnerability to synucleinopathy. NPJ Parkinsons Dis 8, 106. [PubMed: 35982091]

Gass J, et al. , 2012. Progranulin regulates neuronal outgrowth independent of sortilin. Mol. Neurodegener 7, 33. [PubMed: 22781549]

Goldmann T, et al. , 2013. A new type of microglia gene targeting shows TAK1 to be pivotal in CNS autoimmune inflammation. Nat. Neurosci 16, 1618–1626. [PubMed: 24077561]

Gonzalez EM, et al. , 2003. A novel interaction between perlecan protein core and progranulin: potential effects on tumor growth. J. Biol. Chem 278, 38113–38116. [PubMed: 12900424]

Griesbeck O, et al. , 1999. Are there differences between the secretion characteristics of NGF and BDNF? Implications for the modulatory role of neurotrophins in activity-dependent neuronal plasticity. Microsc. Res. Tech 45, 262–275. [PubMed: 10383119]

Gururaj S, et al. , 2020. Progranulin adsorbs to polypropylene tubes and disrupts functional assays: implications for research, biomarker studies, and therapeutics. Front. Neurosci 14, 602235. [PubMed: 33381010]

Holler CJ, et al. , 2017. Intracellular proteolysis of Progranulin generates stable, lysosomal Granulins that are Haploinsufficient in patients with frontotemporal dementia caused by GRN mutations. eNeuro 4.

Hoogland IC, et al. , 2015. Systemic inflammation and microglial activation: systematic review of animal experiments. J. Neuroinflammation 12, 114. [PubMed: 26048578]

Houser MC, et al. , 2022. Progranulin loss results in sex-dependent dysregulation of the peripheral and central immune system. Front. Immunol 13, 1056417. [PubMed: 36618392]

Hu F, et al. , 2010. Sortilin-mediated endocytosis determines levels of the frontotemporal dementia protein, progranulin. Neuron 68, 654–667. [PubMed: 21092856]

Huin V, et al. , 2019. Homozygous GRN mutations: new phenotypes and new insights into pathological and molecular mechanisms. Brain 142, 3636–3654. [PubMed: 31599329]

Hyung S, et al. , 2019. Dedifferentiated Schwann cells secrete progranulin that enhances the survival and axon growth of motor neurons. Glia 67, 360–375. [PubMed: 30444070]

Jacobson I, et al. , 1985. Mass transfer in brain dialysis devices–a new method for the estimation of extracellular amino acids concentration. J. Neurosci. Methods 15, 263–268. [PubMed: 4094481]

Justice JB Jr., 1993. Quantitative microdialysis of neurotransmitters. J. Neurosci. Methods 48, 263–276. [PubMed: 8105154]

Kessenbrock K, et al. , 2008. Proteinase 3 and neutrophil elastase enhance inflammation in mice by inactivating antiinflammatory progranulin. J. Clin. Invest 118, 2438–2447. [PubMed: 18568075]

Kimura A, et al. , 2017. Increased cerebrospinal fluid progranulin correlates with interleukin-6 in the acute phase of neuromyelitis optica spectrum disorder. J Neuroimmunol 305, 175–181. [PubMed: 28100408]

Kleinberger G, et al. , 2016. Reduced secretion and altered proteolytic processing caused by missense mutations in progranulin. Neurobiol. Aging 39 (220), e17–e26.

Krabbe G, et al. , 2017. Microglial NFkappaB-TNFalpha hyperactivation induces obsessive-compulsive behavior in mouse models of progranulin-deficient frontotemporal dementia. Proc. Natl. Acad. Sci. U. S. A 114, 5029–5034. [PubMed: 28438992]

Kurnellas M, et al. , 2023. Latozinemab, a novel progranulin-elevating therapy for frontotemporal dementia. J Transl Med 21, 387. [PubMed: 37322482]

Lang I, et al. , 2018. Lack of evidence for a direct interaction of Progranulin and tumor necrosis factor Receptor-1 and tumor necrosis factor Receptor-2 from cellular binding studies. Front. Immunol 9, 793. [PubMed: 29740434]

Lee MJ, et al. , 2011. rs5848 variant of progranulin gene is a risk of Alzheimer's disease in the Taiwanese population. Neurodegener. Dis 8, 216–220. [PubMed: 21212639]

Lee WC, et al. , 2014. Targeted manipulation of the sortilin-progranulin axis rescues progranulin haploinsufficiency. Hum. Mol. Genet 23, 1467–1478. [PubMed: 24163244]

Lee CW, et al. , 2017. The lysosomal protein cathepsin L is a progranulin protease. Mol. Neurodegener 12, 55. [PubMed: 28743268]

Lui H, et al. , 2016. Progranulin deficiency promotes circuit-specific synaptic pruning by microglia via complement activation. Cell 165, 921–935. [PubMed: 27114033]

Ma Y, et al. , 2017. Progranulin protects hippocampal neurogenesis via suppression of Neuroinflammatory responses under acute immune stress. Mol. Neurobiol 54, 3717–3728. [PubMed: 27215202]

Martens LH, et al. , 2012. Progranulin deficiency promotes neuroinflammation and neuron loss following toxin-induced injury. J. Clin. Invest 122, 3955–3959. [PubMed: 23041626]

Mateo I, et al. , 2013. Reduced serum progranulin level might be associated with Parkinson's disease risk. Eur. J. Neurol 20, 1571–1573. [PubMed: 23398167]

Meeter LH, et al. , 2016. Progranulin levels in plasma and cerebrospinal fluid in Granulin mutation carriers. Dement Geriatr Cogn Dis Extra 6, 330–340. [PubMed: 27703466]

Menzel L, et al. , 2017. Progranulin protects against exaggerated axonal injury and astrogliosis following traumatic brain injury. Glia 65, 278–292. [PubMed: 27778404]

Miyakawa S, et al. , 2020. Anti-sortilin1 antibody up-regulates Progranulin via Sortilin1 Down-regulation. Front. Neurosci 14, 586107. [PubMed: 33384578]

Mohan S, et al. , 2021. Processing of progranulin into granulins involves multiple lysosomal proteases and is affected in frontotemporal lobar degeneration. Mol Neurodegeneration 16, 51.

Morenas-Rodriguez E, et al. , 2016. Progranulin protein levels in cerebrospinal fluid in primary neurodegenerative dementias. J. Alzheimers Dis 50, 539–546. [PubMed: 26682689]

Nalls MA, et al. , 2019. Identification of novel risk loci, causal insights, and heritable risk for Parkinson's disease: a meta-analysis of genome-wide association studies. Lancet Neurol 18, 1091–1102. [PubMed: 31701892]

Naphade SB, et al. , 2010. Progranulin expression is upregulated after spinal contusion in mice. Acta Neuropathol 119, 123–133. [PubMed: 19946692]

Neill T, et al. , 2016. EphA2 is a functional receptor for the growth factor progranulin. J. Cell Biol 215, 687–703. [PubMed: 27903606]

Nicholson AM, et al. , 2014. Progranulin protein levels are differently regulated in plasma and CSF. Neurology 82, 1871–1878. [PubMed: 24771538]

Nicholson AM, et al. , 2016. Prosaposin is a regulator of progranulin levels and oligomerization. Nat. Commun 7, 11992. [PubMed: 27356620]

Perry DC, et al. , 2013. Progranulin mutations as risk factors for Alzheimer disease. JAMA Neurol 70, 774–778. [PubMed: 23609919]

Petkau TL, et al. , 2010. Progranulin expression in the developing and adult murine brain. J. Comp. Neurol 518, 3931–3947. [PubMed: 20737593]

Petkau TL, et al. , 2017a. Conditional loss of progranulin in neurons is not sufficient to cause neuronal ceroid lipofuscinosis-like neuropathology in mice. Neurobiol. Dis 106, 14–22. [PubMed: 28647554]

Petkau TL, et al. , 2017b. Selective depletion of microglial progranulin in mice is not sufficient to cause neuronal ceroid lipofuscinosis or neuroinflammation. J. Neuroinflammation 14, 225. [PubMed: 29149899]

Petoukhov E, et al. , 2013. Activity-dependent secretion of progranulin from synapses. J. Cell Sci 126, 5412–5421. [PubMed: 24046442]

Plowman GD, et al. , 1992. The epithelin precursor encodes two proteins with opposing activities on epithelial cell growth. J. Biol. Chem 267, 13073–13078. [PubMed: 1618805]

Rademakers R, et al. , 2008. Common variation in the miR-659 binding-site of GRN is a major risk factor for TDP43-positive frontotemporal dementia. Hum. Mol. Genet 17, 3631–3642. [PubMed: 18723524]

Reho P, et al. , 2022. GRN mutations are associated with Lewy body dementia. Mov. Disord 37, 1943–1948. [PubMed: 35810449]

Rhinn H, Abeliovich A, 2017. Differential aging analysis in human cerebral cortex identifies variants in TMEM106B and GRN that regulate aging phenotypes. Cell Syst 4, 404–415. [PubMed: 28330615]

Root J, et al. , 2023. Granulins rescue inflammation, lysosome dysfunction, and neuropathology in a mouse model of progranulin deficiency. bioRxiv, 2023.04.17.536004.

Rovelet-Lecrux A, et al. , 2008. Deletion of the progranulin gene in patients with frontotemporal lobar degeneration or Parkinson disease. Neurobiol. Dis 31, 41–45. [PubMed: 18479928]

Ryan CL, et al. , 2009. Progranulin is expressed within motor neurons and promotes neuronal cell survival. BMC Neurosci 10, 130. [PubMed: 19860916]

Saunders A, et al. , 2018. Molecular diversity and specializations among the cells of the adult mouse brain. Cell 174, 1015–1030 e16. [PubMed: 30096299]

Shankaran SS, et al. , 2008. Missense mutations in the progranulin gene linked to frontotemporal lobar degeneration with ubiquitin-immunoreactive inclusions reduce progranulin production and secretion. J. Biol. Chem 283, 1744–1753. [PubMed: 17984093]

Sheng J, et al. , 2014. Progranulin polymorphism rs5848 is associated with increased risk of Alzheimer's disease. Gene 542, 141–145. [PubMed: 24680777]

Shoyab M, et al. , 1990. Epithelins 1 and 2: isolation and characterization of two cysteine-rich growth-modulating proteins. Proc. Natl. Acad. Sci. U. S. A 87, 7912–7916. [PubMed: 2236009]

Smith KR, et al. , 2012. Strikingly different clinicopathological phenotypes determined by progranulin-mutation dosage. Am. J. Hum. Genet 90, 1102–1107. [PubMed: 22608501]

Stirling DR, et al. , 2021. CellProfiler 4: improvements in speed, utility and usability. BMC Bioinformatics 22, 433. [PubMed: 34507520]

Suh HS, et al. , 2012. Regulation of progranulin expression in human microglia and proteolysis of progranulin by matrix metalloproteinase-12 (MMP-12). PLoS One 7, e35115. [PubMed: 22509390]

Takeda S, et al. , 2011. Novel microdialysis method to assess neuropeptides and large molecules in free-moving mouse. Neuroscience 186, 110–119. [PubMed: 21530615]

Tanaka Y, et al. , 2013. Exacerbated inflammatory responses related to activated microglia after traumatic brain injury in progranulin-deficient mice. Neuroscience 231, 49–60. [PubMed: 23201826]

Tang W, et al. , 2011. The growth factor progranulin binds to TNF receptors and is therapeutic against inflammatory arthritis in mice. Science 332, 478–484. [PubMed: 21393509]

Tran ML, et al. , 2023. Cab45 deficiency leads to the mistargeting of progranulin and prosaposin and aberrant lysosomal positioning. Traffic 24, 4–19. [PubMed: 36398980]

Trickler WJ, Miller DW, 2003. Use of osmotic agents in microdialysis studies to improve the recovery of macromolecules. J. Pharm. Sci 92, 1419–1427. [PubMed: 12820146]

Tsien JZ, et al. , 1996. Subregion- and cell type-restricted gene knockout in mouse brain. Cell 87, 1317–1326. [PubMed: 8980237]

Van Damme P, et al. , 2008. Progranulin functions as a neurotrophic factor to regulate neurite outgrowth and enhance neuronal survival. J. Cell Biol 181, 37–41. [PubMed: 18378771]

Vercellino M, et al. , 2011. Progranulin expression in brain tissue and cerebrospinal fluid levels in multiple sclerosis. Mult. Scler 17, 1194–1201. [PubMed: 21613335]

Wang J, et al. , 2010. Pathogenic cysteine mutations affect progranulin function and production of mature granulins. J. Neurochem 112, 1305–1315. [PubMed: 20028451]

Wang BC, et al. , 2015. New discovery rarely runs smooth: an update on progranulin/TNFR interactions. Protein Cell 6, 792–803. [PubMed: 26408020]

Wilke C, et al. , 2016. Serum levels of Progranulin do not reflect cerebrospinal fluid levels in neurodegenerative disease. Curr. Alzheimer Res 13, 654–662. [PubMed: 26971930]

Yamada K, et al. , 2014. Neuronal activity regulates extracellular tau in vivo. J. Exp. Med 211, 387–393. [PubMed: 24534188]

Yin F, et al. , 2010. Exaggerated inflammation, impaired host defense, and neuropathology in progranulin-deficient mice. J. Exp. Med 207, 117–128. [PubMed: 20026663]

Yona S, et al. , 2013. Fate mapping reveals origins and dynamics of monocytes and tissue macrophages under homeostasis. Immunity 38, 79–91. [PubMed: 23273845]

Yu Y, et al. , 2016. Progranulin deficiency leads to severe inflammation, lung injury and cell death in a mouse model of endotoxic shock. J. Cell. Mol. Med 20, 506–517. [PubMed: 26757107]

Zhang Y, et al. , 2014. An RNA-sequencing transcriptome and splicing database of glia, neurons, and vascular cells of the cerebral cortex. J. Neurosci 34, 11929–11947. [PubMed: 25186741]

Zhang J, et al. , 2020. Neurotoxic microglia promote TDP-43 proteinopathy in progranulin deficiency. Nature 588, 459–465. [PubMed: 32866962]

Zhang T, et al. , 2022. Differential regulation of progranulin derived granulin peptides. Mol. Neurodegener 17, 15. [PubMed: 35120524]

Zhang T, et al. , 2023. Progranulin deficiency results in sex-dependent alterations in microglia in response to demyelination. Acta Neuropathol 146, 97–119. [PubMed: 37120788]

Zhou X, et al. , 2015. Prosaposin facilitates sortilin-independent lysosomal trafficking of progranulin. J. Cell Biol 210, 991–1002. [PubMed: 26370502]

Zhou X, et al. , 2017a. Lysosomal processing of progranulin. Mol. Neurodegener 12, 62. [PubMed: 28835281]

Zhou X, et al. , 2017b. Impaired prosaposin lysosomal trafficking in frontotemporal lobar degeneration due to progranulin mutations. Nat. Commun 8, 15277. [PubMed: 28541286]

Zhu J, et al. , 2002. Conversion of proepithelin to epithelins: roles of SLPI and elastase in host defense and wound repair. Cell 111, 867–878. [PubMed: 12526812]

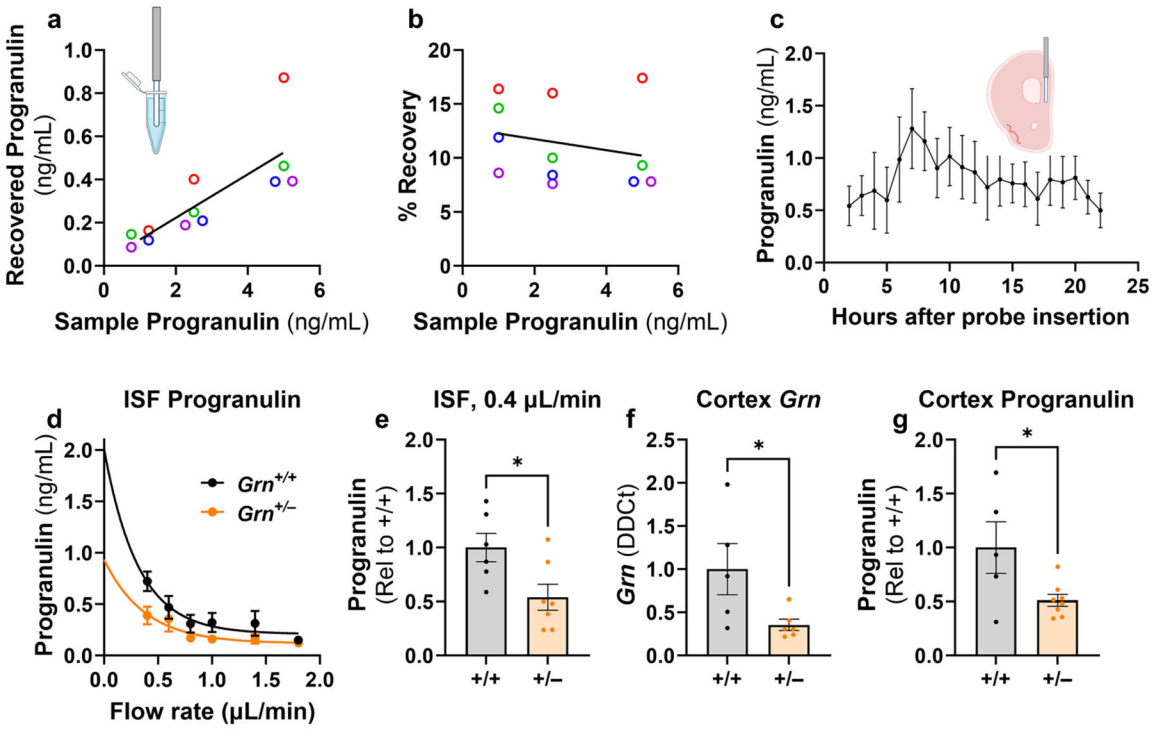

Fig. 1.

Validation of progranulin microdialysis. *in vitro* microdialysis revealed a significant correlation between the concentration of progranulin sampled and the concentration of progranulin recovered by microdialysis (a, Pearson $r = 0.9989$, $p = 0.0301$), but no significant correlation with the concentration of progranulin sampled and the % recovery (b, Pearson $r = 0.5902$, $p = 0.4423$). $n = 4$ probes, each denoted by symbol color.

ISF progranulin recovered by *in vivo* microdialysis stabilized within 8–9 h after probe placement, and typically remained stable for at least 24 h (c shows representative data from 5 mice sampled hourly for 22 h after probe placement). $Grn^{+/-}$ mice exhibited lower levels of ISF progranulin (d, extrapolated extracellular concentration = 2.006 ng/mL for $Grn^{+/+}$ and 0.9339 for $Grn^{+/-}$, e, *t*-test, $p = 0.025$, $n = 6$–8 mice per group). This was consistent with roughly 50% lower *Grn* transcript (f, *t*-test, $p = 0.0445$) and progranulin protein (g, *t*-test, $p = 0.03$) in frontal cortical tissue of $Grn^{+/-}$ mice than wild-type littermates. $n = 5$–8 mice per group. Illustrations in a and c created using Biorender.com.

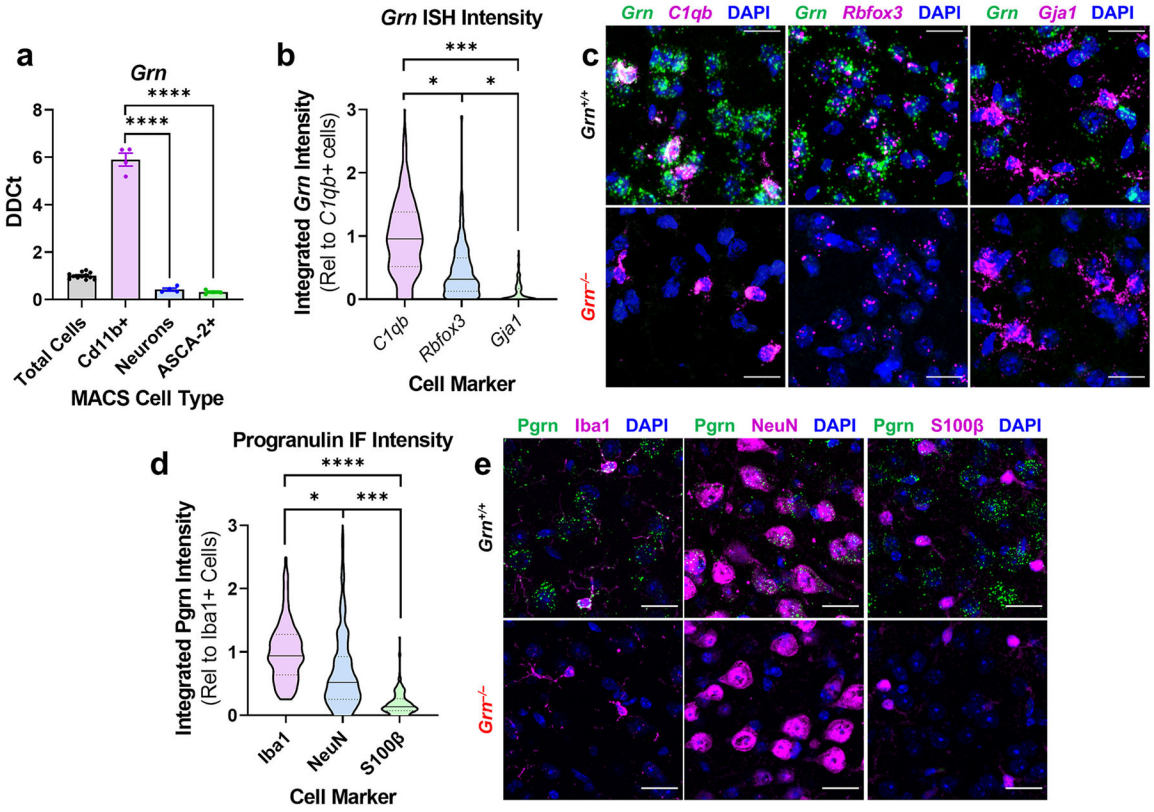

Fig. 2.

Progranulin expression is high in microglia, moderate in neurons, and low in astrocytes. Enrichment of CNS cell types using magnetic activated cell sorting (MACS) revealed high *Grn* transcript levels in microglia (Cd11b+) *versus* neurons (negative selection) and astrocytes (ASCA-2+) (a, ANOVA effect of cell type, $p < 0.0001$, $n = 12$ samples for total cells and 4 samples for each cell type. Each sample was isolated from a single hemibrain from a total of 6 mice.). However, analysis of *Grn* transcript with *in situ* hybridization (ISH) revealed less dramatic differences between microglia and other cell types (b, c). Microglia (*C1qb*+) also exhibited the highest *in situ Grn* expression, with neurons (*Rbfox3*+) exhibiting moderate expression, and astrocytes (*Gja1*+) exhibiting lower expression (b, c, nested ANOVA effect of cell type, $p = 0.0007$, $n = 105$ microglia, 269 neurons, and 94 astrocytes from 3 mice). Analysis of progranulin immunofluorescence (IF) revealed a similar pattern, with microglia (Iba1+) having the highest progranulin immunoreactivity, followed by neurons (NeuN+), then astrocytes (S100β+) (d, e, nested ANOVA effect of cell type, $p < 0.0001$, $n = 149$ microglia, 540 neurons, and 172 astrocytes from 4 mice). Imaging data in b and d were corrected for background fluorescence by subtracting values obtained from $Grn^{-/-}$ mice. Scale bars in c and e represent 20 μm. * = $p <$ 0.05, ** = $p < 0.01$, *** = $p < 0.001$, and **** = $p < 0.0001$ by Tukey's post-hoc test.

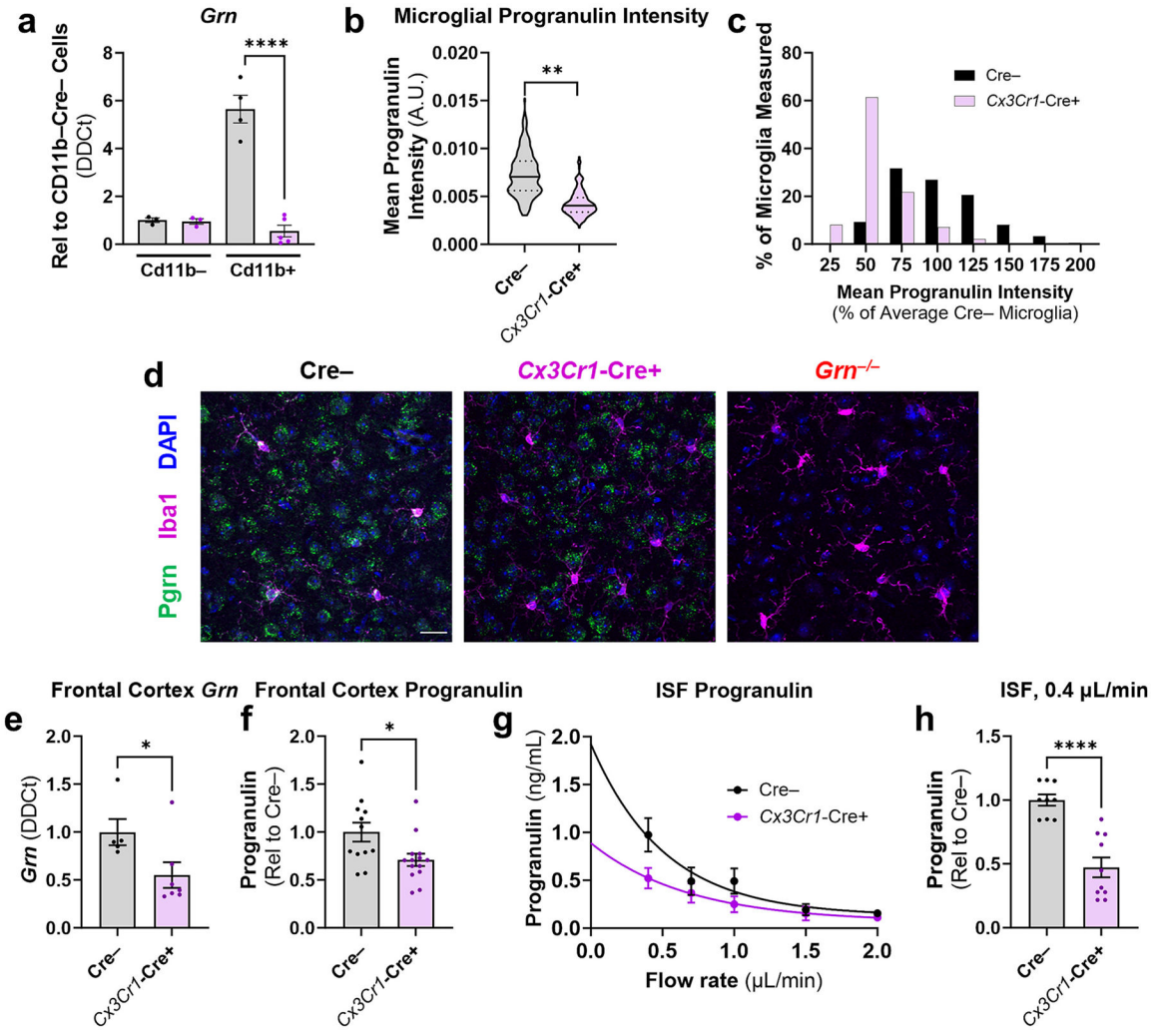

Fig. 3.

Microglia and CNS-resident macrophages are a significant source of ISF progranulin in mPFC. Analysis of Cd11b+ cells isolated by MACS revealed selective depletion of *Grn* transcript in Mg-KO mice (a, ANOVA cell type × Cre interaction, $p < 0.0001$, **** = $p < 0.0001$ by Sidak's post-hoc test $n = 3–5$ samples per group). Similarly, analysis of progranulin immunoreactivity in Iba1+ cells revealed depletion of progranulin in Mg-KO mice (b, nested *t*-test, $p = 0.0099$, $n = 186–199$ cells from 4 mice per genotype). Analysis of the distribution of progranulin intensity revealed that nearly 70% of microglia in Mg-KO mice had less than half the progranulin intensity of the average control microglia (c). Mg-KO mice also exhibited reduction of total *Grn* transcript (e, *t*-test, $p = 0.0463$, $n = 5–7$ mice per group) and progranulin protein (f, *t*-test, $p = 0.019$, n = 12–14 mice per group) in frontal cortex. Mg-KO mice exhibited a roughly 50% decrease in ISF progranulin (g, extrapolated extracellular concentration = 1.923 ng/mL for controls and 0.8885 for Mg-KO, h, *t*-test, $p < 0.0001$, $n = 7–9$ mice per group), indicating that microglia are a significant source of ISF progranulin. Scale bar in d represents 20 µm.

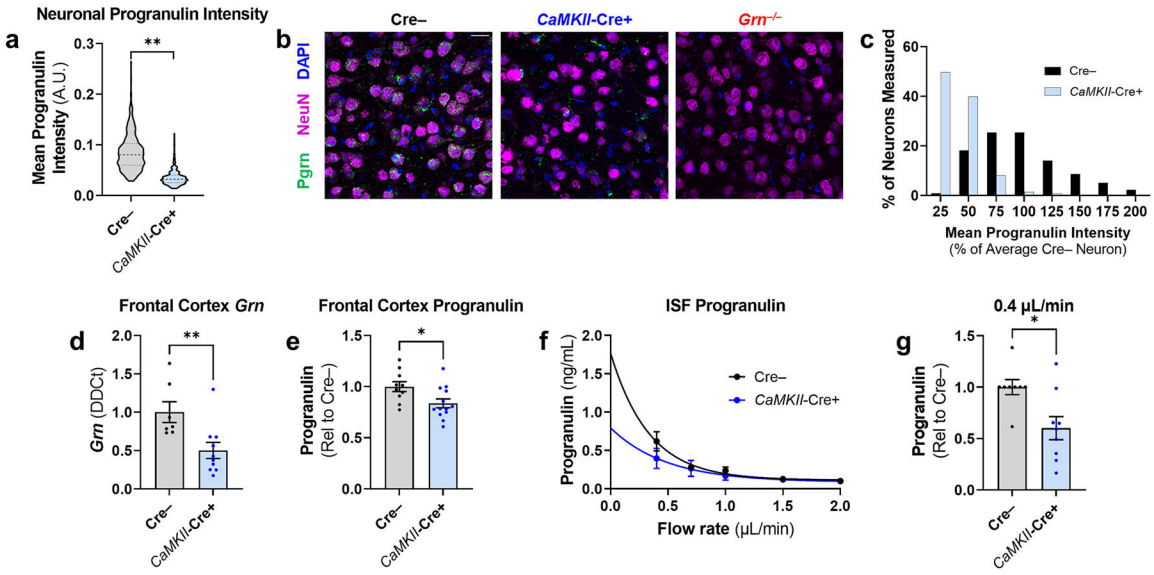

Fig. 4.

Neurons are a significant source of ISF progranulin in mPFC. Analysis of progranulin immunofluorescent intensity in NeuN+ cells revealed depletion of neuronal progranulin in N-KO mice (a, b, nested *t*-test, $p = 0.0022$, $n = 474–487$ cells from 4 mice per genotype). Since *CaMKII*-Cre only targets excitatory neurons, we assessed the distribution of progranulin intensity in NeuN+ cells, and found that nearly 90% of neurons in N-KO mice had less than half the progranulin intensity of the average control neuron (c). Thus, the majority of neurons in mPFC exhibited substantial loss of progranulin immunoreactivity. N-KO mice exhibited reduction of total *Grn* transcript (d, *t*-test, $p = 0.0097$, n = 7–10 mice per group) and progranulin protein (e, *t*-test, $p = 0.0198$, n = 10–13 mice per group) in frontal cortex. N-KO mice also exhibited a roughly 50% decrease in ISF progranulin (f, extrapolated extracellular concentration = 1.766 ng/mL for controls and 0.7936 for N-KO, g, *t*-test, $p = 0.011$, $n = 8–9$ mice per group), indicating that excitatory neurons are also a significant source of ISF progranulin. Scale bar in b represents 20 µm.

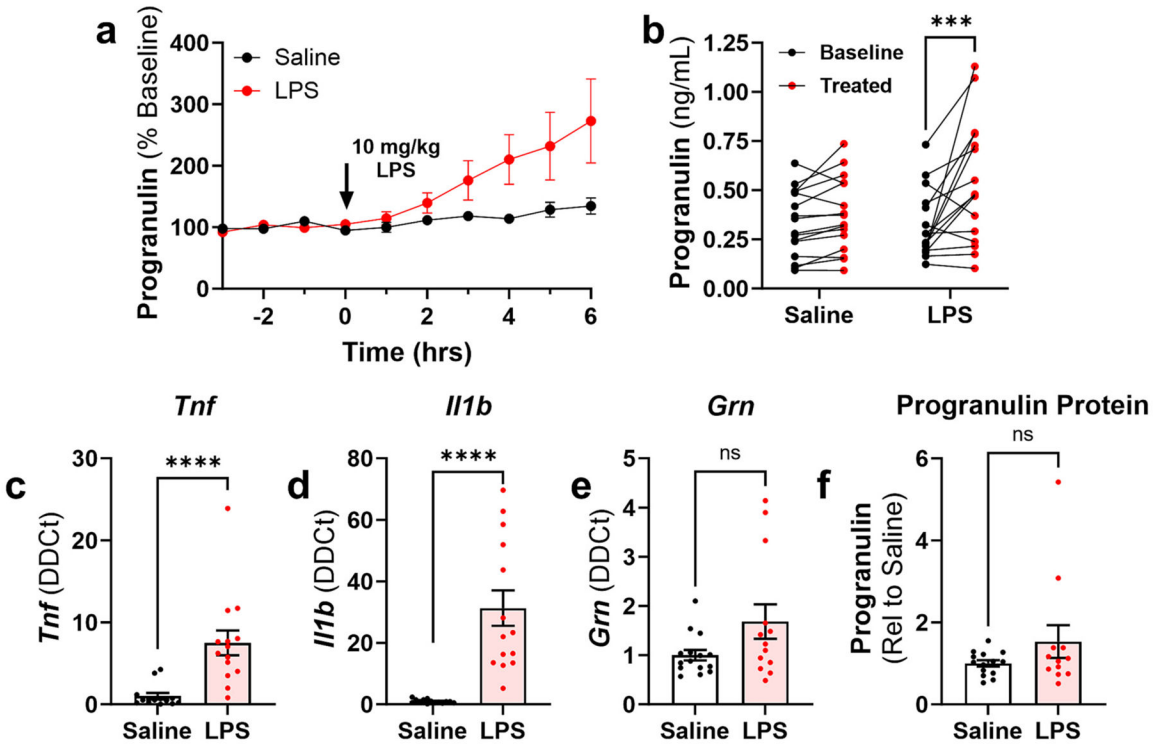

Fig. 5.

Induction of inflammation with LPS increases ISF progranulin in mPFC. Mice injected with 10 mg/kg LPS, i.p. (arrow in a) exhibited an increase in ISF progranulin in the mPFC over the six hours following injection (a, Mixed effects analysis effect of LPS, $p = 0.0425$, time × LPS, $p = 0.0003$, b, RM ANOVA time × LPS, $p = 0.0268$, *** = $p < 0.001$ by Sidak's post-hoc test, $n = 16$ mice per group). LPS produced a robust increase in *Tnf* (c, *t*-test, $p < 0.0001$, $n = 13$–14 mice per group) and *Il1b* (d, *t*-test, $p < 0.0001$, n = 14 mice per group), but failed to significantly increase *Grn* transcript (e, *t*-test, $p = 0.0885$, n = 13–15 mice per group) or progranulin protein (f, *t*-test, $p = 0.2457$, n = 12–14 mice per group) in the contralateral frontal cortex.

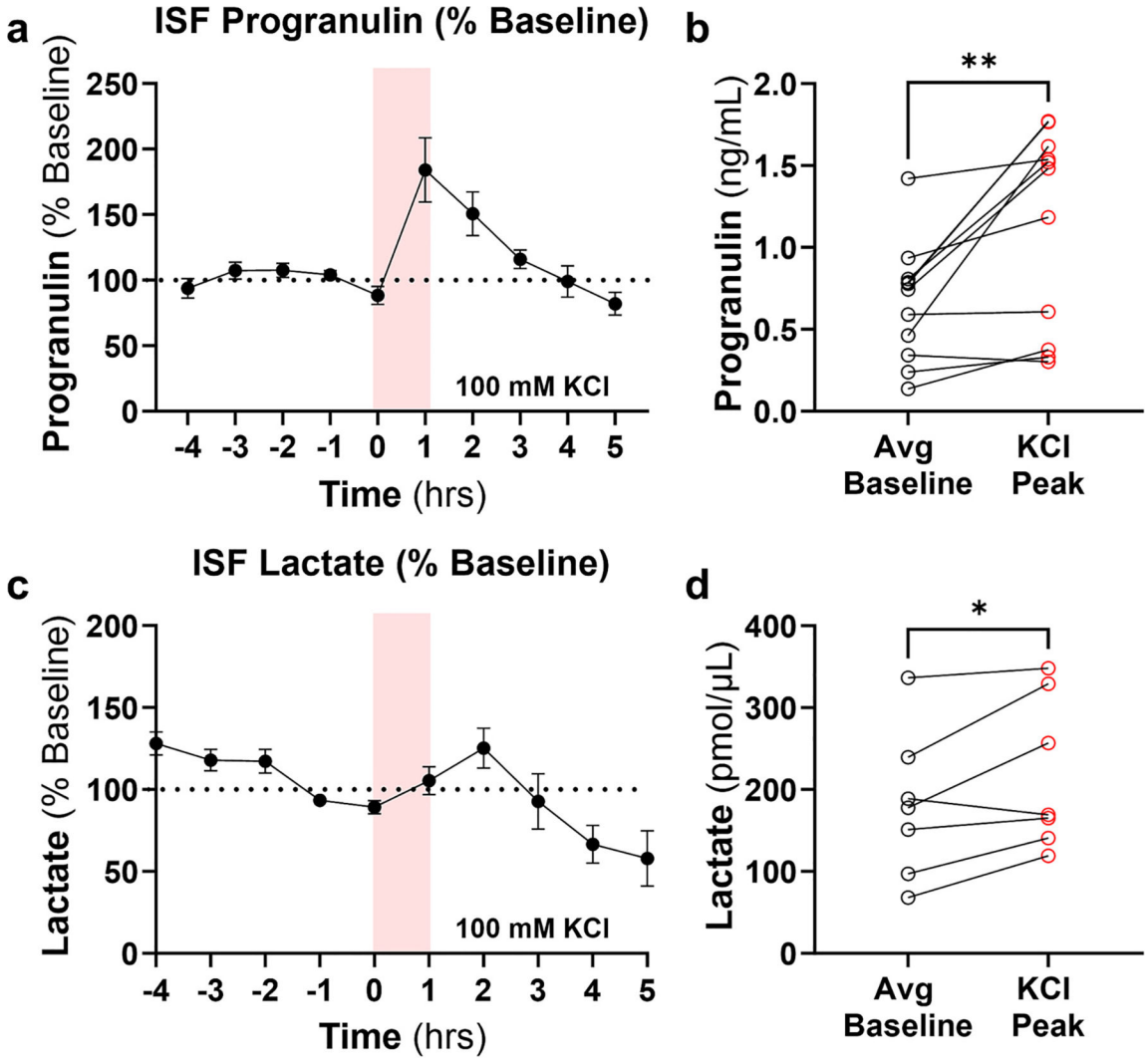

Fig. 6.

Cellular depolarization increases ISF progranulin in mPFC. Infusion of aCSF containing 100 mM KCl produced an immediate increase in ISF progranulin that returned to baseline over the next few hours (a, mixed effect analysis effect of time, $p = 0.0019$, b, paired t-test, $p = 0.0051$, $n = 11$ mice). Stimulation of metabolic activity was confirmed by an increase in ISF lactate after KCl infusion (c, mixed effects analysis effect of time, $p = 0.0087$, d, paired t-test, $p = 0.0408$, n = 7 mice).

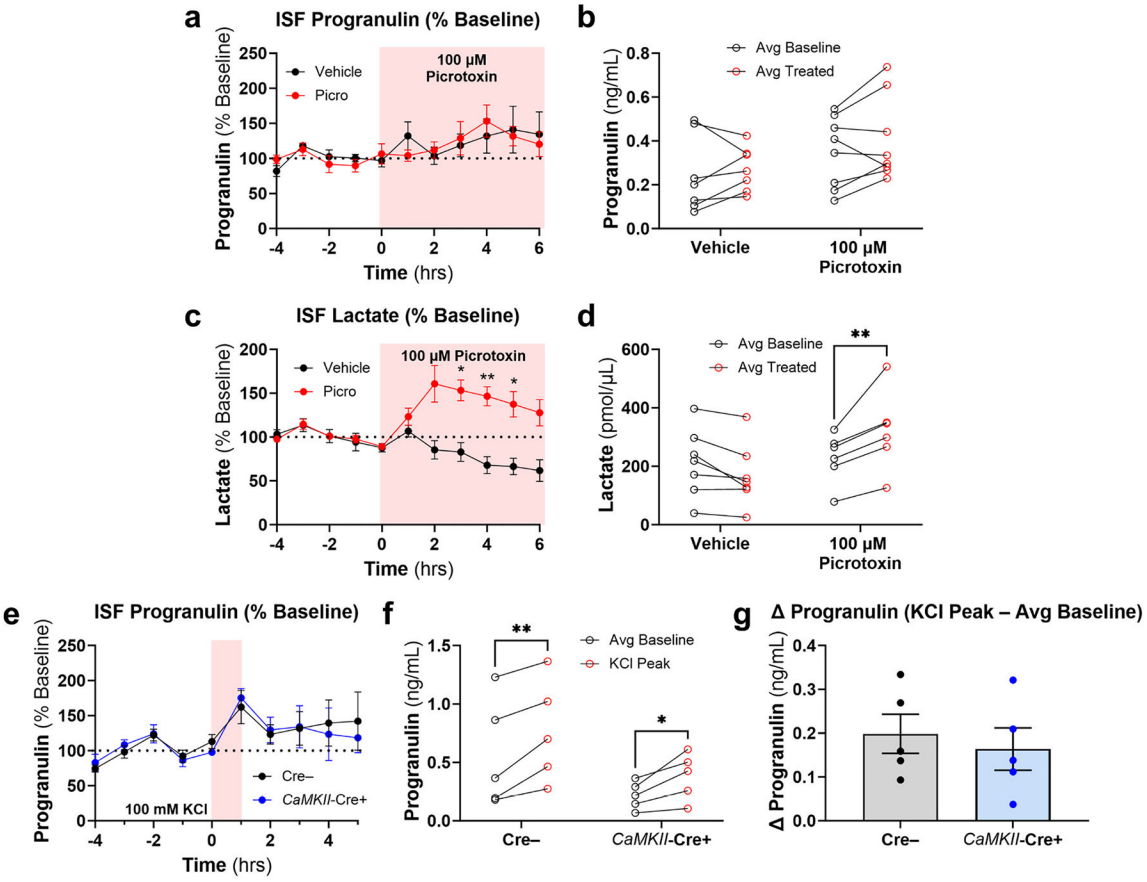

Fig. 7.

Neuronal activity does not increase ISF progranulin in mPFC. Stimulating neuronal activity by infusion of 100 µm picrotoxin did not increase ISF progranulin (a, repeated measures ANOVA effect of picrotoxin, $p = 0.9341$, time × picrotoxin, $p = 0.8395$, b, repeated measures ANOVA effect of picrotoxin, $p = 0.2708$, time × picrotoxin, $p = 0.4795$, $n = 6–8$ mice per group). This was not due to a failure to stimulate neuronal activity, as picrotoxin robustly increased lactate levels in ISF (c, repeated measures ANOVA effect of picrotoxin, $p < 0.0001$, time × picrotoxin, $p < 0.0001$, * = $p < 0.05$, ** = $p < 0.01$ by Sidak's post-hoc test, d, repeated measures ANOVA time × picrotoxin, $p = 0.0006$, ** = $p < 0.01$ by Sidak's post-hoc test, n = 6–7 mice per group). Infusion of aCSF containing 100 mM KCl produced a similar increase in progranulin in N-KO mice and control littermates (e, mixed effects analysis effect of time, $p = 0.0217$, effect of Cre, $p = 0.9434$, time × Cre, $p = 0.9923$, f, repeated measured ANOVA effect of KCl, $p = 0.0006$, * = $p < 0.05$ and ** = $p < 0.01$ by Sidak's post-hoc test, n = 5 mice per genotype), and the change in progranulin concentration from baseline did not differ between control and N-KO mice (g, *t*-test, $p = 0.6099$).